

Adhesive energy and charge transfer for MgO/Cu heterophase interfaces

R. Benedek

Department of Materials Science and Engineering, Northwestern University, Evanston, Illinois 60208

M. Minkoff

Mathematics and Computer Science Division, Argonne National Laboratory, Argonne, Illinois 60439

L. H. Yang

Condensed Matter Physics Division, Lawrence Livermore National Laboratory, University of California, Livermore, California 94551

(Received 10 April 1996)

Local-density-functional-theory (LDFT) calculations within the plane-wave pseudopotential framework are performed for two polar (111) and two nonpolar (100) MgO/Cu interfaces. The polar interfaces have larger works of adhesion than nonpolar ones, consistent with field-ion and electron-microscopy observations of (111) interfaces in internally oxidized specimens. Large shifts in the potential of the interface layer relative to the bulk occur in the polar but not in the nonpolar interfaces. For both polar and nonpolar interfaces, the charge transfer profile is essentially confined to two layers on each side of the interface. [S0163-1829(96)07735-1]

Ceramic-metal interfaces¹ play a prominent role, for example, in metal-matrix composites, supported catalysts, oxide scales on high-temperature alloys, and electronic packaging. There is considerable interest in developing an atomic-scale description of such interfaces to guide the tailoring of interfacially controlled properties. Atomistic modeling of ceramic-metal interfaces, however, is less developed than that of grain boundaries,² owing largely to the lack of convenient yet realistic interatomic-force models. An approach based on image-charge interactions complemented by suitable short-range interatomic forces across the ceramic-metal interface has been explored.³⁻⁵ Although such cohesive models incorporate some aspects of the chemical bonding at ceramic-metal interfaces, other bonding effects, such as charge transfer and covalency, are omitted, and the metallic side of the interface is typically treated as a continuum in image-charge formulations. More rigorous, but much more computationally intensive, are local-density-functional theory (LDFT) calculations, e.g., for alumina/Nb,⁶ CdO/Ag,⁷ and MgO/metal interfaces (references to Table I). Non-self-consistent tight-binding calculations have also been performed.⁸

A fundamental property of ceramic-metal interfaces is the work of adhesion, W (or the interface energy, related to it for nonpolar interfaces by the Dupré equation⁹). Considerable attention has been given to the calculation of metal adhesion to the MgO(100) substrate (cf. Table I). Existing results suggest the importance of a self-consistent electronic structure calculation for the accurate prediction of interface properties even for this relatively inert substrate; the desirability of self-consistent treatment is at least equally great for noninert, polar interfaces, such as MgO/Cu(111). No quantitative comparisons exist, however, between polar and nonpolar ceramic-metal interfaces.

We explore in this work the differences between polar and nonpolar MgO/Cu interfaces by an *ab initio* treatment. MgO/Cu(111) interfaces are known experimentally to be chemically¹⁰ and structurally¹¹ sharp. Four MgO/Cu inter-

faces are considered: (111) polar interfaces with Mg or O terminations, and two different nonpolar (100) interface configurations. The polar interfaces are found to be more strongly bonded than nonpolar ones, which may explain the absence of the latter in MgO precipitates grown by internal oxidation in a Cu matrix.¹²

The charge-transfer profile¹³ $\delta n(z) \equiv n(z) - n_s(z)$ [where $n(z)$ is the average valence-electron density in a plane at distance z from the interface and $n_s(z)$ is the superposition of the metal and the ceramic charge densities in the absence of the interface] gives a compact description of the interface charge distribution. $\delta n(z)$ is significantly nonzero over a width of 3–4 Å for all of the interfaces considered, slightly wider than the interface separation, although small-amplitude charge-density oscillations extend deeper into the bulk metal. This localization of $\delta n(z)$ suggests that short-range interatomic potentials, calibrated by LDFT total-energy calculations, may enable modeling of the interactions across the interface to reasonable accuracy. With such potentials, large-scale atomistic simulations that include the ceramic-metal misfit would become feasible.

Our calculations employ the plane-wave pseudopotential representation of local-density-functional theory. The resultant Kohn-Sham equations are solved with a conjugate-gradient algorithm,¹⁴ stabilized for metallic systems by a charge-density-mixing procedure.¹⁵ Soft-core pseudopotentials¹⁶ in separable form are used in conjunction with Gaussian-broadened energy levels,¹⁷ and special k -point¹⁸ sampling. Minimal special k -point sets are employed in most cases (for example, three k points for the polar interfaces) but tests were run to verify the relative insensitivity of adhesive energies to k -point sampling. A basis-set energy cutoff of 70 Ry is adopted.¹⁶ For each interface, the unit cell includes several layers each of MgO and Cu, with either one or two atoms per layer. With the adopted periodic boundary conditions, interfaces may be simulated with either a periodic-slab or a multilayer geometry. In the periodic-slab geometry, each cell contains a single interface,

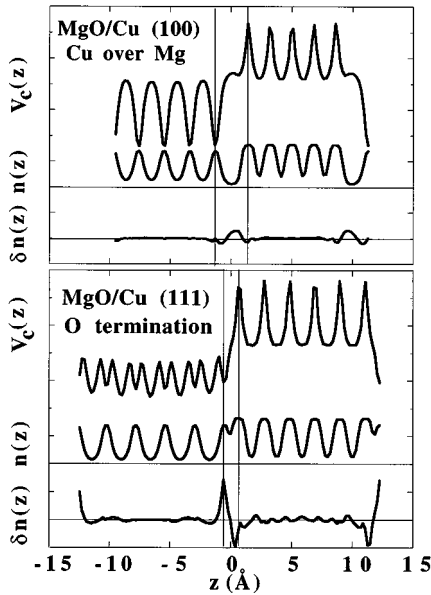


FIG. 1. Planar-averaged valence-electron density profile $n(z)$, charge-transfer profile $\delta n(z)$, and effective Coulomb potential $V_c(z)$ for the MgO/Cu O-terminated (111) (lower panel) and the Cu-over-Mg (100) interface (upper panel). The ceramic (metal) is at negative (positive) z . Vertical lines denote the ceramic and the metal interface layers. The scale of $n(z)$ is such that the integral between successive minima in the bulk is 11 electrons per atom per layer. The scale for $\delta n(z)$ is magnified by a factor of 20 relative to that for $n(z)$. The interval between major and minor ordinate ticks corresponds to 10 eV for $V_c(z)$.

and two free surfaces, whereas the multilayer geometry has two interfaces per cell, and space is fully occupied. Clearly, neither geometry exactly replicates an interface between semi-infinite solids; however, features common to calculations performed with both types of unit cell can reasonably be regarded as interface-related. Such consistency checks are most germane for polar interfaces, since spurious supercell-dependent electric fields¹⁹ are more likely to occur in the presence of charged layers. Concerns about such artifacts may have discouraged previous treatments of polar (111)

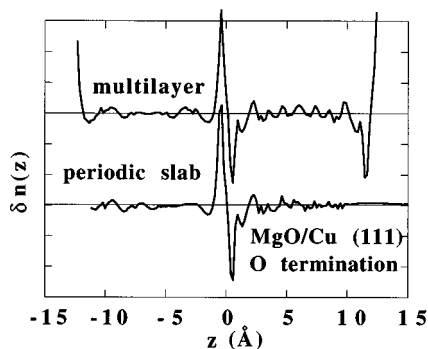


FIG. 2. $\delta n(z)$ for MgO/Cu O-terminated (111) interface, calculated with the periodic-slab geometry (lower curve), and the multilayer geometry (displaced vertically for clarity).

ceramic-metal interfaces. Several tests have therefore been performed for the (111) interface with O termination. Results for the adhesive energy, interface separation, and charge transfer are similar for the periodic slab and multilayer geometries.

The mismatch (≈ 15 percent) between the lattice constants of MgO and Cu, is known to be accommodated by a misfit-dislocation network that bounds individual coherent domains.¹² Since our calculations treat a Cu in-plane lattice constant stretched to that of MgO, the results may be regarded as describing the coherent regions between the misfit dislocations.²⁰ The primitive unit cell for an ideal coherent interface contains only a single atom of a given species per layer.

Works of adhesion are obtained by subtraction of total energies at equilibrium from those at large interface separation. The calculated works of adhesion are listed in Table I, along with published results for other MgO/metal interfaces. In agreement with previous LDFT results for (100) interfaces, we find the atop-O configuration favored over the atop-Mg one (image-charge models²¹ find the interstitial configuration the most stable.) The larger W for MgO/Cu (100) than MgO/Ag(100) is consistent with the rule of proportionality²² between the stability of MgO/M and that of the metal oxide MO. LDFT calculations²³ for adsorption of Cu atoms on MgO(100) are in accord with our calculations, giving slightly larger binding energies, and shorter bond lengths than the present results for solid-solid adhesion.

Existing calculations for MgO/M are exclusively for non-polar (100) interfaces. The present calculations show that MgO/Cu(111) interfaces of either termination are more stable than (100) interfaces. One obvious reason for the enhanced stability is the geometry (where, e.g., an interface Cu lies above a triangle of O atoms), which enables multiple bonding across the interface. Calculated results for several properties are plotted in Fig. 1 for the most stable [O-terminated (111)] interface (lower panel) and for the least stable [(100) with Cu over Mg] interface (upper panel). The ceramic (metal) layers are at negative (positive) z . In the lower panel, peaks in the valence electron density profile $n(z)$ correspond to the O and Cu layers, and Mg layers lie at the minima between the O layers; in the upper panel peaks in $n(z)$ correspond to MgO layers. The locations of the interface layers are denoted by vertical lines. Below the density profile is the charge-transfer profile $\delta n(z)$ (scaled by a factor of 20). We note that for both interfaces $\delta n(z)$ is non-negligible only in the vicinity of the interface bilayer, i.e., near $z=0$.²⁴ In fact, except at the interfaces, the integrated valence electron charge between adjacent minima are $8e$ in MgO and $11e$ in Cu, to within about $0.01e$, so that local neutrality holds, except for the interface and immediately adjacent layers.

In the lower panel, we find that the maximum (minimum) in $\delta n(z)$ occurs in the vicinity of the O (Cu) interface layer, which implies electron transfer from Cu to O. The magnitude of charge transfer, which we define as the integrated density under the peak of $\delta n(z)$, is $0.18e$. The charge transfer for (100)(Cu over Mg) (upper panel) is considerably smaller ($0.06e$), and the transfer is essentially from the ceramic to the metal, opposite to the behavior in the lower panel.

TABLE I. Calculated MgO/metal interface separation, works of adhesion and charge transfers. Calculations for MgO/Cu (100) interfaces are performed in the multilayer geometry with (5|5) (MgO|Cu) layers. Calculations for the (111) O- or Mg-terminated interfaces are performed for the periodic slab geometry with (3,3|3), and (5,5|5) (Mg,O|Cu) layers, and for the multilayer geometry with (3,4|5) and (5,6|6) layers. Periodic slabs are separated by 6.2 Å gap. Some previously published calculations for MgO/metal interfaces are listed for comparison. Calculations by Li *et al.* (Ref. 23) are for adsorbed Cu atoms, and by Li *et al.* (Ref. 25) for a Ag monolayer; the other entries are based on several metal layers.

M (oriented)	Configuration	Interface Separation (bond length) (Å)	W (eV)	Charge transfer (e)	Author(s)
Cu(111)	O terminated	1.25 (2.1)	2.9	0.18	This work
Cu(111)	Mg terminated	2.1 (2.7)	1.7	0.15	This work
Cu(100)	over O	2.0 (2.0)	1.0	0.08	This work
Cu(100)	over Mg	2.6 (2.6)	0.2	0.06	This work
Cu(100)	over O	1.9 (1.9)	1.4		Li <i>et al.</i> (Ref. 23)
Cu(100)	over Mg	2.5 (2.5)	0.5		Li <i>et al.</i> (Ref. 23)
Ag(100)	over O	2.7 (2.7)			Li <i>et al.</i> (Ref. 25)
Ag(100)	over O	2.34 (2.34)	1.05		Smith <i>et al.</i> (Ref. 26)
Ag(100)	over O	2.49 (2.49)	0.88		Schönberger <i>et al.</i> (Ref. 27)
Ag(100)	over Mg		0.4		Schönberger <i>et al.</i> (Ref. 27)
Ag(100)	over O	2.38 (2.38)	0.54		Duffy <i>et al.</i> (Ref. 21)
Al(100)	over O	2.02 (2.02)	0.61		Smith <i>et al.</i> (Ref. 26)
Ti(100)	over O	2.18 (2.18)	1.2		Schönberger <i>et al.</i> (Ref. 27)

Small oscillations occur in $\delta n(z)$ deeper into the bulk on the metallic ($+z$) side of the polar (111) interface. That these oscillations represent the electronic response to the interface (and not artifacts) is shown in Fig. 2, in which $\delta n(z)$ calculated for a periodic slab may be compared with that for the multilayer geometry (also plotted in the lower panel of Fig. 1). The structural features in $\delta n(z)$ for $z < 5$ Å are similar for both geometries (Since the multilayer cell possesses a symmetry plane in the vicinity of $z = 5$ Å no correspondence exists for larger z .)

The uppermost curves in each panel of Fig. 1 are the effective Coulomb potentials, V_c , including the contribution of the local (but not the nonlocal) pseudopotential. The atomic planes lie at maxima (minima) in V_c for the metal (ceramic) layers. The strong interface perturbation shifts the potential of the O layer at the interface relative to the bulk layers in the lower panel, whereas virtually no shift occurs for the interface MgO plane in the upper panel. This potential shift, as well as pd hybridization at the interface, displaces the positions of the O local-density-of-electronic-states features (not shown) associated with the $2p$ bands towards higher energy at the interface, relative to the bulk, for the polar (111) interface, whereas no such shift is observed for the nonpolar (100) interfaces.

The analysis of $\delta n(z)$ for the two interfaces not represented in Fig. 1 yields charge transfers of $0.08e$ for the (100)(Cu over O) interface, and $0.15e$ for the Mg-terminated (111) interface. Charge transfers for the four interfaces are collected in Table I.

In summary, we present *ab initio* calculations for polar and nonpolar ceramic-metal interfaces between cubic materials. Several significant differences are found between the

polar and nonpolar interfaces. The polar interfaces exhibit (i) larger works of adhesion and charge transfers, (ii) stronger hybridization (not discussed in detail in this paper), (iii) larger shifts in the interface layer potentials relative to the bulk, than the nonpolar interfaces, and (iv) small amplitude electronic-density oscillations extending at least 5 Å into the metal. The region of large nonzero charge transfer density $\delta n(z)$, however, is only slightly greater than the interface separation, for both polar and nonpolar interfaces.

The results appear to explain the observation of (111), rather than (100), ceramic-metal interfaces for MgO precipitates in internally oxidized Cu specimens.^{10–12} The potential shifts at the interface layer for the polar interfaces may manifest themselves, e.g., in electron-energy-loss or x-ray spectra as O($2p$) core level shifts. The relatively short range of $\delta n(z)$ suggests that the interface interactions may be adequately modeled for atomistic simulations by short-range interatomic potentials.

We thank M. W. Finnis for helpful correspondence. R. B. is grateful to D. N. Seidman for support and encouragement. He was supported by the U.S. Department of Energy, Basic Energy Sciences under Grant No. DE FG02ER45403/06. R. B. also acknowledges the hospitality of the Materials Science Division, Argonne National Laboratory. M. M. was supported by the Office of Computational and Technology Research of the U.S. Department of Energy under Contract No. W-31-109-ENG-38. L. H. Y. was supported by the U.S. Department of Energy under Contract No. W-7405-ENG-48. Most of the computational work was performed at the National Energy Research Supercomputer Center.

- ¹*Metal-Ceramic Interfaces*, edited by M. Rühle, A. G. Evans, M. F. Ashby, and J. P. Hirth (Pergamon, Oxford, 1990); *Proceedings of the International Symposium on Metal-Ceramic Interfaces*, edited by M. Rühle *et al.* [Acta Metall. Mater. **S40**, (1992)].
- ²*Materials Interfaces: Atomic-level Structure and Properties*, edited by D. Wolf and S. Yip (Chapman and Hall, London, 1994); A. P. Sutton and R. W. Balluffi, *Interfaces in Crystalline Materials* (Clarendon Press, Oxford, 1995).
- ³A. M. Stoneham and P. W. Tasker, J. Phys. C **18**, L543 (1985).
- ⁴D. M. Duffy, J. H. Harding, and A. M. Stoneham, Acta Metall. Mater. **43**, 1559 (1995).
- ⁵M. W. Finnis, Acta Metall. Mater. **40**, S25 (1992).
- ⁶C. Kruse, M. W. Finnis, V. Y. Milman, M. C. Payne, A. de Vita, and M. J. Gillan, J. Am. Ceram. Soc. **77**, 431 (1994), and unpublished.
- ⁷F. Rao, R. Wu, and A. J. Freeman, Phys. Rev. B **51**, 10 052 (1995).
- ⁸See, for example, P. Alemany, R. S. Boorse, J. M. Burlitch, and R. Hoffmann, J. Phys. Chem. B **97**, 8464 (1993).
- ⁹J. M. Howe, Int. Mater. Rev. **38**, 236 (1993).
- ¹⁰D. A. Shashkov and D. N. Seidman, Phys. Rev. Lett. **75**, 268 (1995); H. Jang, D. N. Seidman, and K. L. Merkle, Int. Sci. **1**, 61 (1993).
- ¹¹P. Lu and F. Cosandey, Ultramicrosc. **40**, 271 (1992); F. R. Chen *et al.*, *ibid.* **54**, 179 (1994).
- ¹²Only oxygen-terminated MgO/Cu interfaces have been observed, (Ref. 10) in contrast to CdO/Ag [D. K. Chan, D. N. Seidman, and K. L. Merkle, Phys. Rev. Lett. **75**, 1118 (1995)] for which roughly equal numbers of anion- and cation-terminated (111) interfaces were found.
- ¹³R. Benedek, A. P. Smith, and L. H. Yang, Phys. Rev. B **49**, 7786 (1994).
- ¹⁴M. P. Teter, M. Payne, and D. G. Allan, Phys. Rev. B **40**, 12 255 (1989).
- ¹⁵R. Benedek, L. H. Yang, C. Woodward, and B. I. Min, Phys. Rev. B **45**, 2607 (1992).
- ¹⁶N. Troullier and J. L. Martins, Phys. Rev. B **43**, 1993 (1991).
- ¹⁷C. L. Fu and K.-M. Ho, Phys. Rev. B **28**, 5480 (1983).
- ¹⁸H. J. Monkhorst and J. D. Pack, Phys. Rev. B **13**, 5188 (1976).
- ¹⁹J. Neugebauer and M. Scheffler, Phys. Rev. B **46**, 16 067 (1992).
- ²⁰To compare calculated works of adhesion with experiment, results for perfectly coherent interfaces must be corrected for misfit dislocations and elastic strain; see, e.g., Hong *et al.* (Ref. 24).
- ²¹D. M. Duffy, J. H. Harding, and A. M. Stoneham, Philos. Mag. A **67**, 865 (1993).
- ²²K. H. Johnson and S. V. Pepper, J. Appl. Phys. **53**, 6634 (1982).
- ²³Y. Li, D. C. Langreth, and M. R. Pederson, Phys. Rev. B **52**, 6067 (1995).
- ²⁴The localization of $\delta n(z)$ is consistent with previous results for nonpolar interfaces, e.g., T. Hong, J. R. Smith, and D. J. Srolovitz, J. Adhes. Sci. Tech. **8**, 837 (1994).
- ²⁵C. Li, R. Wu, A. J. Freeman, and C. L. Fu, Phys. Rev. B **48**, 8317 (1993).
- ²⁶J. R. Smith, T. Hong, and D. J. Srolovitz, Phys. Rev. Lett. **72**, 4021 (1994).
- ²⁷U. Schönberger, O. K. Andersen, and M. Methfessel, Acta Metall. Mater. B **40**, S1 (1992).